

Biosystems Engineering

An unsupervised automatic measurement of wheat spike dimensions in dense 3D point clouds for field application --Manuscript Draft--

Manuscript Number:	YBENG-D-21-00168R4
Article Type:	SI: Biosystems and Metrology
Keywords:	k-means, point clouds, shape-fitting, unsupervised algorithm, wheat phenotype
Corresponding Author:	Fuli Wang University of Essex UNITED KINGDOM
First Author:	Fuli Wang
Order of Authors:	Fuli Wang Fengping Li Vishwanathan Mohan Richard Dudley Dongbing Gu Ruth Bryant
Manuscript Region of Origin:	Europe
Abstract:	<p>An accurate measurement of field-grown wheat traits, including spike number, dimension and volume are essential for crop phenotyping and yield analysis. A high-throughput method to image field-grown wheat in three dimensions is presented with an accompanying unsupervised measuring method to obtain individual wheat spike data. Images are captured using four structured light scanners on a field mobile platform, creating dimensionally accurate sub-millimetre resolution 3D point clouds for a 4.5 m³ volume in less than 10 s. The unsupervised method analyses each trial plot's 3D point cloud, containing hundreds of wheat spikes, calculating the average size of the wheat spike and total spike volume per plot. The analysis utilises an adaptive k-means algorithm with dynamic perspectives, to fit each spike's shape and measures the dimensions with a random sample consensus algorithm. The method generates small cuboids to fit all the wheat spikes and estimate the total spikes volume. Experimental results show that the proposed algorithm is a reliable tool for identifying spikes from wheat crops and identifying individual spikes. Compared with the manual measurement, according to the results of five scenes, the average error rate in the number of spikes, spikes' height and spikes' width in tests were 16.27%, 5.24% and 12.38% respectively.</p>
Suggested Reviewers:	Yifeng Li Peking University liyifeng@pku.edu.cn
Opposed Reviewers:	
Response to Reviewers:	

Declaration of interests

The authors declare that they have no known competing financial interests or personal relationships that could have appeared to influence the work reported in this paper.

The authors declare the following financial interests/personal relationships which may be considered as potential competing interests:

An unsupervised automatic measurement of wheat spike dimensions in dense 3D point clouds for field application

Highlights

- Laser imaging technology for automatic field phenotyping application.
- High-throughput field capture platform was constructed.
- Unsupervised algorithm allows for wheat dimensions measurement in 3D point clouds.
- Automatic measurement can estimate wheat spike size, volume and number of spikes.
- Framework was evaluated by comparing the experiment with manual measurement.

An unsupervised automatic measurement of wheat spike dimensions in dense 3D point clouds for field application

Fuli Wang ^{a,*}, Fengping Li ^b, Vishwanathan Mohan ^a, Richard Dudley ^b, Dongbing Gu ^a, Ruth Bryant ^c

^a School of Computer Science and Electronic Engineering, University of Essex, Colchester, United Kingdom

^b National Physical Laboratory, Hampton Road, Teddington, Middlesex, United Kingdom

^c RAGT Seeds Ltd, Grange Road, Ickleton, Essex, United Kingdom

Abstract

An accurate measurement of field-grown wheat traits, including spike number, dimension and volume are essential for crop phenotyping and yield analysis. A high-throughput method to image field-grown wheat in three dimensions is presented with an accompanying unsupervised measuring method to obtain individual wheat spike data. Images are captured using four structured light scanners on a field mobile platform, creating dimensionally accurate sub-millimetre resolution 3D point clouds for a 4.5 m³ volume in less than 10 s. The unsupervised method analyses each trial plot's 3D point cloud, containing hundreds of wheat spikes, calculating the average size of the wheat spike and total spike volume per plot. The analysis utilises an adaptive *k*-means algorithm with dynamic perspectives, to fit each spike's shape and measures the dimensions with a random sample consensus algorithm. The method generates small cuboids to fit all the wheat spikes and estimate the total spikes volume. Experimental results show that the proposed algorithm is a reliable tool for identifying spikes from wheat crops and identifying individual spikes. Compared with the manual measurement, according to the results of five scenes, the average error rate in the number of spikes, spikes' height and spikes' width in tests were 16.27%, 5.24% and 12.38% respectively.

Keywords: *k*-means, point clouds, shape-fitting, unsupervised algorithm, wheat phenotype

Nomenclature

2D	Two-dimensional
3D	Three-dimensional
RANSAC	Random sample consensus
DBSCAN	Density-based spatial clustering of applications with noise

RGB	Red Green Blue
CAD	Computer-aided design
Alg. 1	Algorithm 1: Obtaining wheat spikes
Alg. 2	Algorithm 2: Adaptive k -means algorithm based on dynamic perspectives
$Error_1$	Error rate in the number of spikes
$Error_2$	Error rate in the spike height
$Error_3$	Error rate in the spike width

1. Introduction

Plant phenotyping is a vital tool for the development of new crop varieties and requires the undertaking of many trial growth programmes, measuring and analysing trait variations over many seasons. Accurate and repeatable trait measurement is essential for success in phenotyping application. The major phenotypes for wheat breeding are the number of spikes, spike length/wide and volume. However, data collection of spike size is still primarily conducted with manual sampling (Torres & Pietragalla, 2012). A number of techniques have been explored for collecting data for quantitative studies of complex traits related to the growth, yield and adaptation to biotic or abiotic stress (see (Lei Li et al., 2014) and references therein). Spike counting is one of the main approaches for predicting grain yield in wheat and other cereals (Pask et al., 2012). To count the number of wheat spikes, Deery et al., (2014) used a simple particle count algorithm on segmented 2D images but was unable to address the challenge of high crop density and overlapping spikes. Reducing count errors in dense, close contact spikes was explored by Fernandez-Gallego et al., (2018), using an automatic spike-counting algorithm and zenithal colour 2D images of the crop in natural light conditions. Algorithms such as DeepCount (Sadeghi-Tehran et al., 2019; Tan et al., 2020) have been developed to count the number of wheat spikes in 2D images using the deep convolutional neural networks and machine learning approaches. Achieving volumetric or dimensional information is challenging, especially when taken from directly above or from an angle where distortions are introduced and only partial visibility mask the real size of the spike. Calibration charts can mitigate distortions and mosaicking errors, but there are complex to implement for high-throughput field studies.

Generating a 3-D, digital twin of a wheat plot offers a much richer and dimensional correct representation, overcoming issues of obscured and overlapping spikes. Generating the digital twin is achieved by combining multiple 2D images or utilising more complex imaging technology such as Lidar, time-of-flight or structured light scanners (Mohamed & Dudley, 2019). The field captured data is no longer represented by a 2D RGB image but a 3D point cloud with format

27 $P_n(x, y, z, RGB)$. Algorithms used for 2D image analysis are no longer applicable for point
28 clouds and alternative approaches have been developed using supervised neural networks to fit
29 complex geometric primitives, such as CAD models of mechanical components (Lingxiao Li et
30 al., 2019; Su et al., 2018). However, by using a more classical clustering algorithm to segment
31 the wheat, and then subsequently fitting to spikes, the process of training a supervised model can
32 be omitted, and the fitting results can be obtained with less time cost. For example, Velumani et
33 al., (2017) performed wheat spike segmentation using two different classical methods: voxel-
34 based segmentation and mean shift segmentation. Additionally, density-based spatial clustering
35 of applications with noise (DBSCAN) algorithm (Ester et al., 1996) has been developed for the
36 task of segmentation, and then least-squares curve fitting is used to obtain the size of the wheat
37 spikes (Thompson et al., 2019). Although the clustering algorithms such as DBSCAN, mean
38 shift and k -means can be successful in segmentation tasks, the segmentation task can be chal-
39 lenging for these algorithms in specific complex environments, such as when wheat crops are
40 very dense. Our recent work has proposed an adaptive k -means algorithm with dynamic perspec-
41 tives, which performs segmentation to separate the wheat spikes, to tackle this challenge (Wang
42 et al., 2020). Although this algorithm can be applied in an environment where multiple wheat
43 spikes are grown densely, it still cannot address more than one hundred wheat spikes. As shown
44 in Fig. 1, compared with sample wheat crops in lab, the captured 3D point cloud images from
45 the field usually have hundreds of spikes and can contain noise, which makes it difficult for the
46 existing measurement algorithms to obtain a robust measurement result. This paper contributes
47 to filling this gap by providing an unsupervised framework to tackle 3D point cloud images with
48 hundreds of wheat crops from the field.

49 To realise the field application, the proposed k -means algorithm needs to separate the wheat
50 spikes, remove the stems and then obtain the spikes. Since there are hundreds of wheat spikes,
51 the method randomly selects some areas as sample areas and calls the adaptive k -means algo-
52 rithm to calculate the average spike size. Meanwhile, the algorithm segments all of the spikes as
53 thousands of small segments and uses cuboids to fit each segment and estimate the total volume
54 of all spikes. The number of wheat spikes can be approximately estimated according to the av-
55 erage size and total volume. The proposed method is described in detail in section 3.

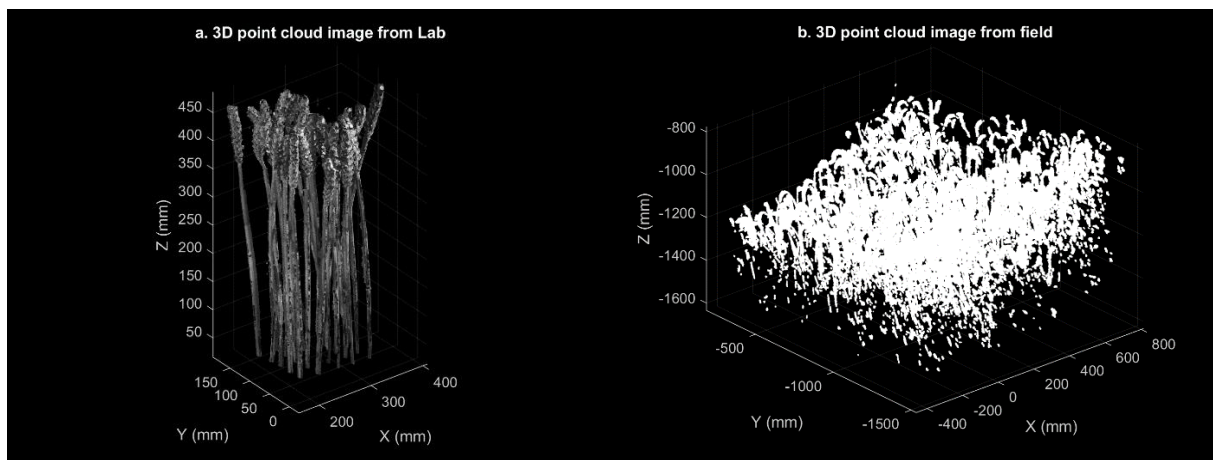


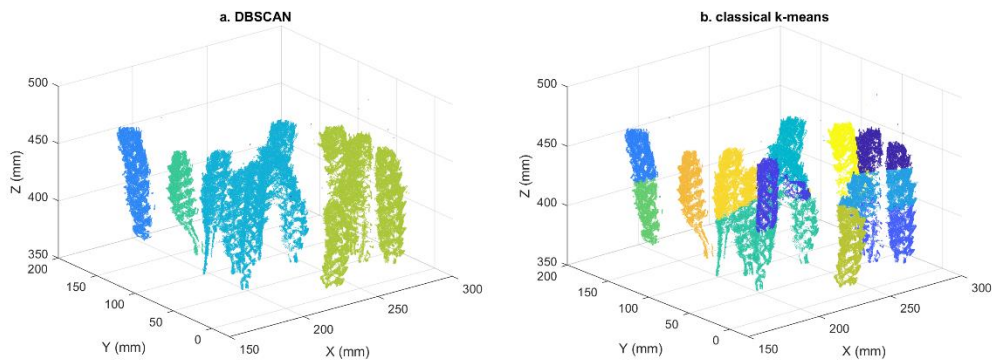
Fig. 1 - 3D point cloud images of wheat crops.

2. The adaptive k -means algorithm with dynamic perspectives

2.1. Classical clustering algorithms

The clustering algorithms are useful tools for the task of separating spikes from wheat crops in the point cloud. As discussed in the introduction, there are not many complex geometric primitives in wheat crops. The DBSCAN and k -means algorithms are well suited to the task, but some defects still exist when dealing with some practical situations. One of the disadvantages of the DBSCAN is that the performance depends largely on the selection of parameters, but there is no theoretical guidance for setting its parameters. Therefore, the trial method is used commonly, but it relies on experience, which results in the final parameters not necessarily being optimal (Lai et al., 2019). However, k -means has the characteristics of a single parameter, and its parameter k represents the cluster number. To compare these two classical algorithms, Fig. 2 demonstrates the segmentation results of the DBSCAN (*the minimum number of neighbours is set as 10, the neighbourhood radius is set as 5*) and classical k -means ($k = 12$). As there are 12 spikes, we set the parameter of k -means as 12 and used the trial method to set the relatively reasonable parameters of the DBSCAN. The DBSCAN algorithm can only roughly divide the 12 spikes into four segments; in other words, DBSCAN identifies that there are only four spikes (with different colours in Fig. 2a), which is quite different from the actual situation. Meanwhile, in the classical

75 *k*-means algorithm, even if we set the number of clusters to 12, the output result is still not satis-
 76 factory. These narrow results illustrate that the classical clustering algorithm cannot handle some
 77 complex environments such as when wheat crops are very dense.

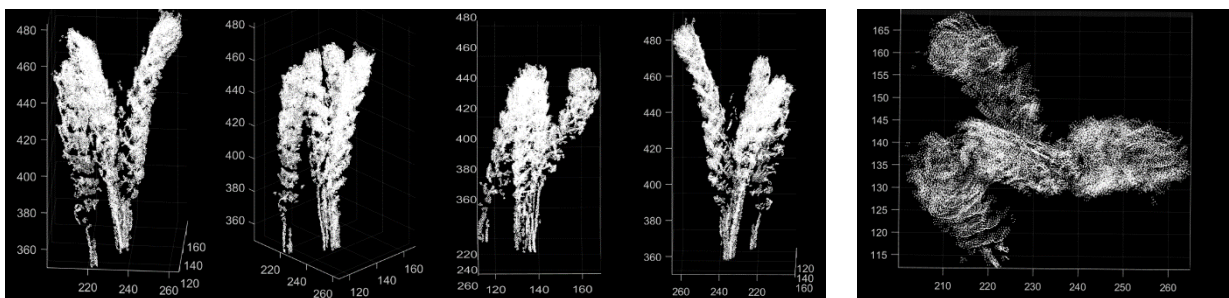


78
79

Fig. 2 - Results of DBSCAN and classical *k*-means segmentation.

80 2.2. The *k*-means algorithm based on dynamic perspectives

81 To address the above concerns, the adaptive *k*-means algorithm with dynamic perspectives
 82 was used. To demonstrate this idea, as is shown in Fig. 3, when wheat crops are observed from
 83 the side, which part is the wheat spike and which part is the stem can be easily distinguished.
 84 Due to overlapping between the spikes, how many spikes cannot be easily judged from the side
 85 view (Fig. 3a). However, the top view can be used to count the number of spikes (Fig. 3b).
 86 Similarly, for the *k*-means algorithm, if all of the 3D points are projected into the 2D top view,
 87 the point distance in the within-cluster is reduced and clustering performance will be improved.



88

a) Side views

b) Top view

89

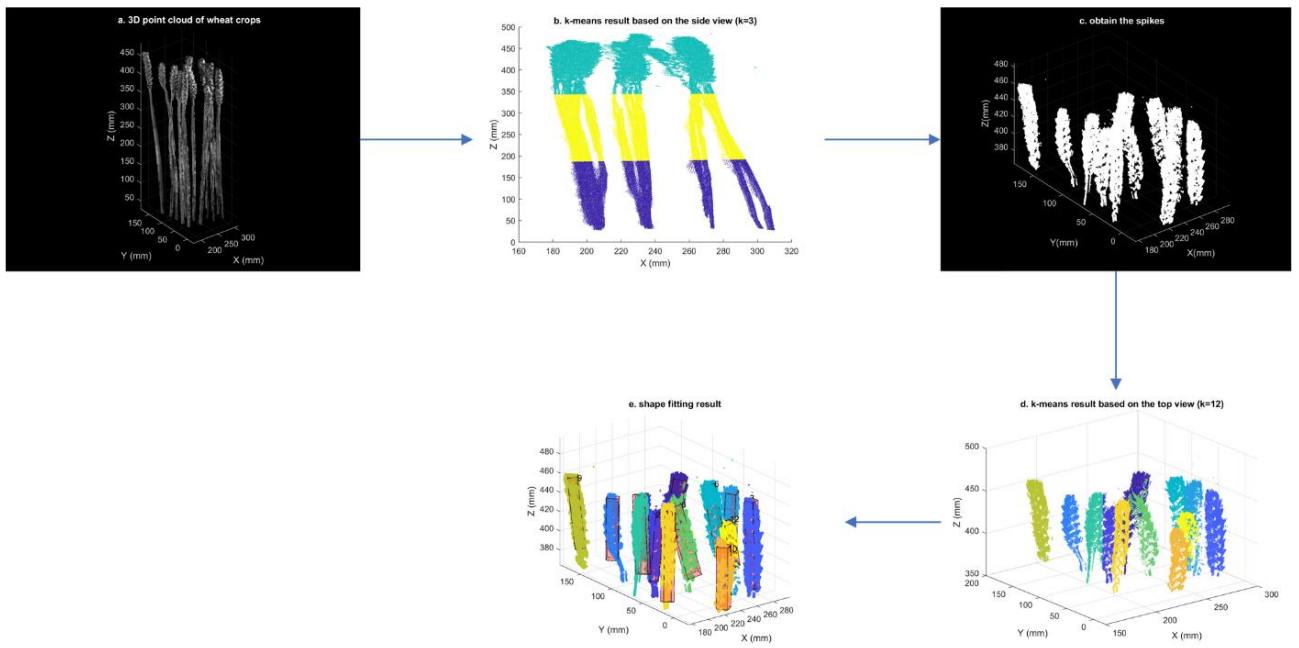
Fig. 3 - The spikes observation with dynamic perspectives.

90

91 To improve segmentation performance, the above idea was introduced into the *k*-means
 92 algorithm. The flowchart of the *k*-means algorithm with dynamic perspectives can be seen in Fig.

93 4. Specifically, given a cluster consisting of points $N_{n \times 3}$ (Fig. 4a), where n is the number of
94 points, and 3 is the number of dimensions, we denote by $\{x_i\}$, $\{y_i\}$ and $\{z_i\}$ the x , y and z
95 coordinates of the point $i (i \in n)$. For the side view, we transfer the $N_{n \times 3}$ array into an $N_{n \times 2}$ array,
96 which only contains the two dimensions of $\{x_i\}$ and $\{z_i\}$. The 2D points were inputted from
97 the side view into the k -means, which outputs all point labels. Using the labels to mark all 3D
98 points, the clustering result in Fig. 4b were achieved. **To separate spikes from the wheat (Fig.**
99 **4c), Algorithm 1 (Alg. 1) is defined to preserve the top segments.** Similarly, transferring the 3D
100 points of spikes into the top view $N'_{n \times 2}$, which only contains two dimensions of $\{x_i\}$ and $\{y_i\}$,
101 we obtain the segmentation result based on the top view in Fig. 4d, which is better than the
102 classical algorithms results. Finally, a random sample consensus (RANSAC) algorithm
103 (Schnabel et al., 2007) was used to fit each segment shape and obtain the dimensions as shown
104 in Fig. 4e.

105 In Alg. 1 defined below, a value space according to the highest point of all 3D points was
106 defined which has the max value of $\{Z\}$. By extracting all the segments in the value space, the
107 points belonging to spikes are obtained. As is shown in Fig.5, the highlighted area is the value
108 space which is determined by the parameter σ . Once this value space was defined, to preserve
109 the top segments, only whether the highest point of each segment is located in this space was
110 required. By using this operation to preserve the top segments, the space value does not have to
111 be set too accurately; it is sufficient to ensure that σ is a small value (Fig. 5a and Fig. 5b are
112 both the correct spaces that can output the same result). Note that, if we change the conditional
113 statement in Alg.1 to judge whether the lowest point of each segment is located in this space, the
114 σ would be set to a larger value (in the case of Fig. 5c). In this paper, the former conditional
115 statement (with σ set to 60 mm) was used and use statistical filtering reduced the noise.



116
117
118

Fig. 4 - Segmentation results base on the proposed k -means.

Algorithm 1: Obtaining wheat spikes

Require: 3D points: $N_{n \times 3}$;

Initialize parameter of σ ;

Reduce the noises of 3D points;

Obtain side view 2D points: $N_{n \times 3} \rightarrow N_{n \times 2}$

Use the k -means for segmentation based on side view;

Obtain the point with the highest Z coordinate value: Z_{\max} ;

Calculating a value space of Z coordinates:

$$\left[Z_{\max} - \sigma, Z_{\max} \right]$$

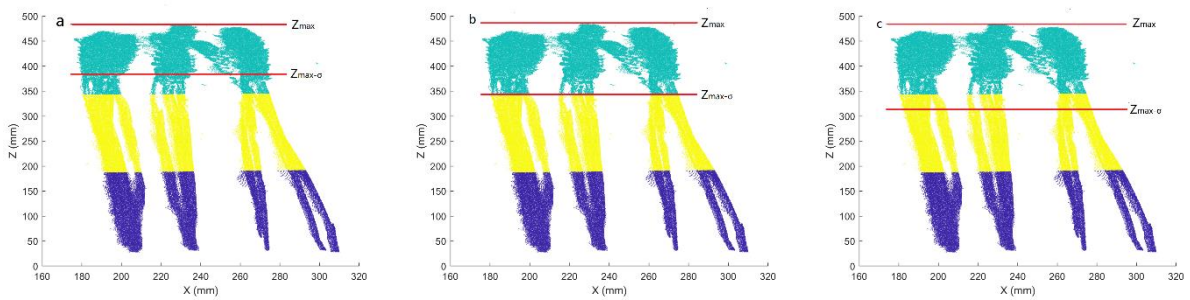
For each highest point within its segment:

If the highest point is located in the value space: Preserve this segment

else: continue;

return all preserved segments.

119



120

121 **Fig. 5 – Three different value spaces for spikes obtaining. From a to c , the value σ gradually increases.**

122 As can be seen from Fig. 4, it is sufficient to set the k -means parameter to 3 or 4 for the side
123 view. Since the shape of the wheat crop is similar to a cuboid or cylinder, selecting the side view
124 from the X or Y direction will obtain the same final result. Further, shape fitting for each spike
125 is required with the number of clusters set in advance, that is, the number of spikes. In Fig. 4, k
126 was set to 12 for the top view. However, in practical application, it is impossible to know how
127 many wheat spikes there are in advance. This means that it was expected that the algorithm can
128 calculate the number of spikes by itself. To realise this function, this paper adds an adaptive
129 operation to self-update the appropriate parameter values. The detail of this adaptive k -means
130 algorithm based on dynamic perspectives is described in Alg. 2.

131 In the algorithm, an initial parameter k' is required to perform the segmentation for the top
132 view. The value of this initial parameter should be a small number as the algorithm can update
133 it adaptively. In this paper, to set the initial value, DBSCAN provided by Rolf Harkes, (2018)
134 was used which makes use of the k - d trees spatial partitioning algorithm, because the DBSCAN
135 can roughly divide the spikes into a few segments, which is far smaller than the actual number
136 of spikes. After obtaining the initial parameter k' , the algorithm uses k -means to segment the 2D
137 points of the top view and then calls the RANSAC algorithm to fit a cuboid to each segmentation.
138 Since the initial value of k' is small, the fitting result is not accurate. As is shown in Fig. 6a,
139 when the k' is small, some abnormal spike sizes will be outputted (the fitting size of the purple
140 part is significantly larger than that of regular wheat). Therefore, once the algorithm detects un-
141 reasonable results, the k' will be superimposed until a reasonable final result is outputted (Fig.
142 6b). The last updated k' value is the number of spikes counted by the algorithm.

Algorithm 2: Adaptive k -means algorithm based on dynamic perspectives

```

Obtain the wheat spikes according to Alg.1
Set the initial parameter  $k'$  for the top view
Obtain top view 2D points:  $N'_{n \times 3} \rightarrow N'_{n \times 2}$ 

```

```

repeat

```

```

    Use the  $k$ -means for segmentation based on top view;

```

```

    Use RANSAC to fit each segment;

```

```

    Evaluate the size of each segment;

```

```

    if (there is an abnormal size)

```

```

         $k'++$ ;

```

```

        break;

```

```

    end if

```

```

until there is no abnormal size

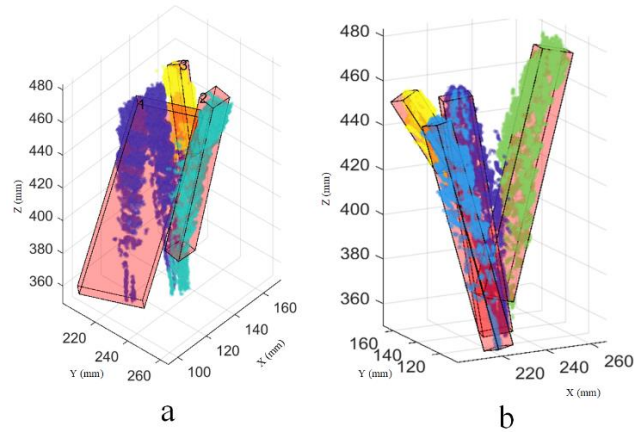
```

```

return the updated shape model.

```

143



144

145 **Fig. 6 - (a) The shape fitting result with abnormal sizes ($k' = 3$); (b) the final shape fitting result ($k' = 4$).**

146 Note that the algorithm did not make any intrinsic change to the k -means algorithm, and
147 instead, it required several iterations of any existing implementation of k -means. Therefore, the
148 algorithm can call any version of the k -means algorithm. Considering the computational perfor-
149 mance, it is recommended to use Lite k -means (Cai, 2011) or ball k -means (Xia et al., 2020) to
150 run the proposed algorithm.

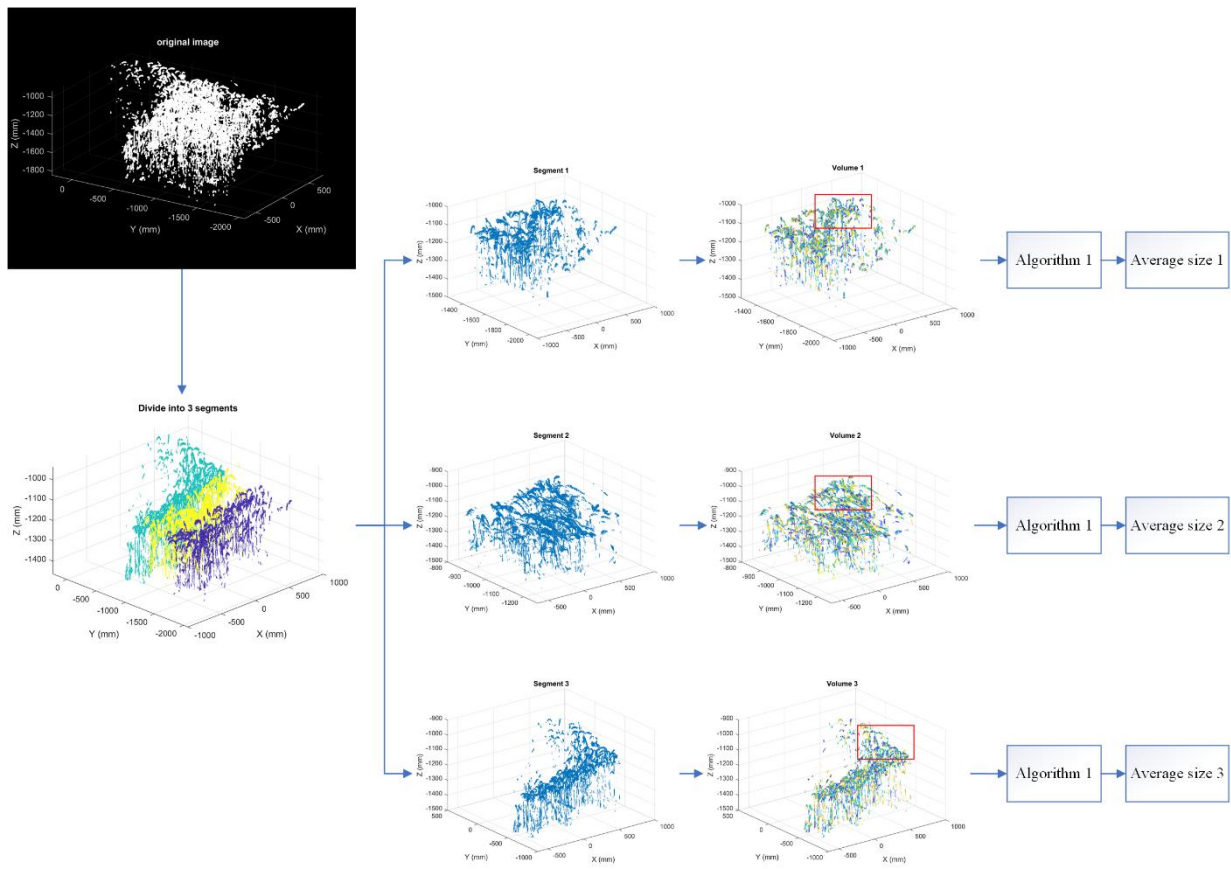
151 3. The framework of the proposed method for wheat field application

152 Although Alg. 2 can deal with the environment where multiple wheat spikes are grown
153 densely better than classical algorithms, it is still challenging to directly apply Alg.2 with images
154 captured over a wide area such as shown in Fig. 1b. Suppose we directly use Alg.2 to deal with

155 these images, as there are so many noises and wheat crops, the computational efficiency will be
156 significantly reduced. Besides, due to noise interference, it is difficult to output an ideal result
157 without abnormal size.

158 To address the above problem, as is shown in Fig. 7, our proposed method was extended
159 based on Alg. 2. Firstly, the original field image was divided into a few segments, and some
160 stems are removed. As can be seen in Fig. 7, the original image was divided into three segments,
161 then the spikes volume of each segment was calculated separately. To calculate the volume,
162 3,000 small cuboids were used to fit the shape of all spikes for each segment. There is an illus-
163 tration to show the volume calculation method in Fig. 8; in this example, there are 50 cuboids to
164 realise the shape fitting of 3 spikes, so the volume of spikes is the sum of the volumes of all
165 cuboids. After the volume calculation, some small areas were selected as sample areas (the red
166 highlighted areas in Fig. 7), then Alg. 2 was used to calculate the average size of these areas.
167 Overall, for images from the wheat field, the total spikes volume and the average size of a single
168 spike could be estimated by the proposed method.

169 The above description involves two parameters. The first is the number of segments and the
170 second is the number of small cuboids. In this paper, all of the original images were divided into
171 3 segments and 3,000 cuboids used to deal with each segment. If the value of these parameters
172 increases, the accuracy of the calculation results might be improved, but it would also increase
173 the calculation cost.



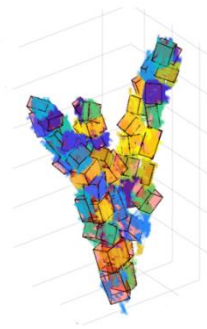
$$\text{Average size of wheat} = (\text{Average size 1} + \text{Average size 2} + \text{Average size 3}) / 3$$

$$\text{Total volume of all spikes} = \text{Volume 1} + \text{Volume 2} + \text{Volume 3}$$

174

175

Fig. 7 - Overall flowchart of the proposed method.



176

177

Fig. 8 – An example of volume calculation method by using cuboids fitting.

178 **4. 3D Field Capture**

179 Imaging technologies applicable for field capture include time-of-flight cameras, structured
180 light scanners, and stereo RGB. To understand the performance of each system a series of com-
181 missioning tests were undertaken (Mohamed & Dudley, 2019). Our aim was to construct a port-
182 able, field-deployable solution that could completely image a field-grown trial plot, dimension
183 2 x 5 x 1 m, in less than one second ready for analysis with wheat identification algorithms. The
184 platform had to be easily moved between plots, deal with typical weather conditions including
185 direct solar illumination and be self-powered. The solution deployed in the fields during 2020 is
186 shown in Fig. 9, which included four structured light scanners from Photoneo (**Photoneo s.r.o.,**
187 **Bratislava, Slovakia**) each positioned parallel to one side of the trial plot edge and orientated at
188 45° to the vertical. The arrangement ensured the capture of the central region of the plot only
189 neglecting 300 mm around the edges which are normally excluded from analysis in most trials.
190 Each scanner was triggered in sequence to avoid interference and a region of 2 x 2 x 1.5 m was
191 captured in approximately 5 s. The scanners were optimised to overcome bright ambient light
192 using structural netting above and to the sides of the mounting frame, but also critical was the
193 selection of the scanner's exposure, laser brightness and processing algorithms.



194
195

Fig. 9 – Field use of 3D capture system incorporating 4 Photoneo L scanners.

196 Reconstructing the four independent Photoneo scans into a single point cloud was achieved
197 using a common reference chart placed in view of all scanners, this is just visible in Fig. 9. Unlike
198 single point measurement systems, our final point clouds include information of the complete
199 surface for all the wheat heads with detail down to grain level. The final point clouds were
200 cleaned for noise using a statistical outlier filter and the resolution was reduced with a sub-sam-
201 pling algorithm to reduce the computational power needed for the next stage of processing, iden-
202 tifying spikes and performing dimensional measurements.

203 In total 25 trial plots were captured over three hours with delays primarily caused by phys-
204 ical movement of the platform around rows, failed captures from wind motion and some data
205 management tasks not yet fully automated. However, with further optimisations, it was estimated
206 that a single platform of this type would be able to capture between 100 and 250 trial plots per
207 working day.

208 **5. Experimental results and discussion**

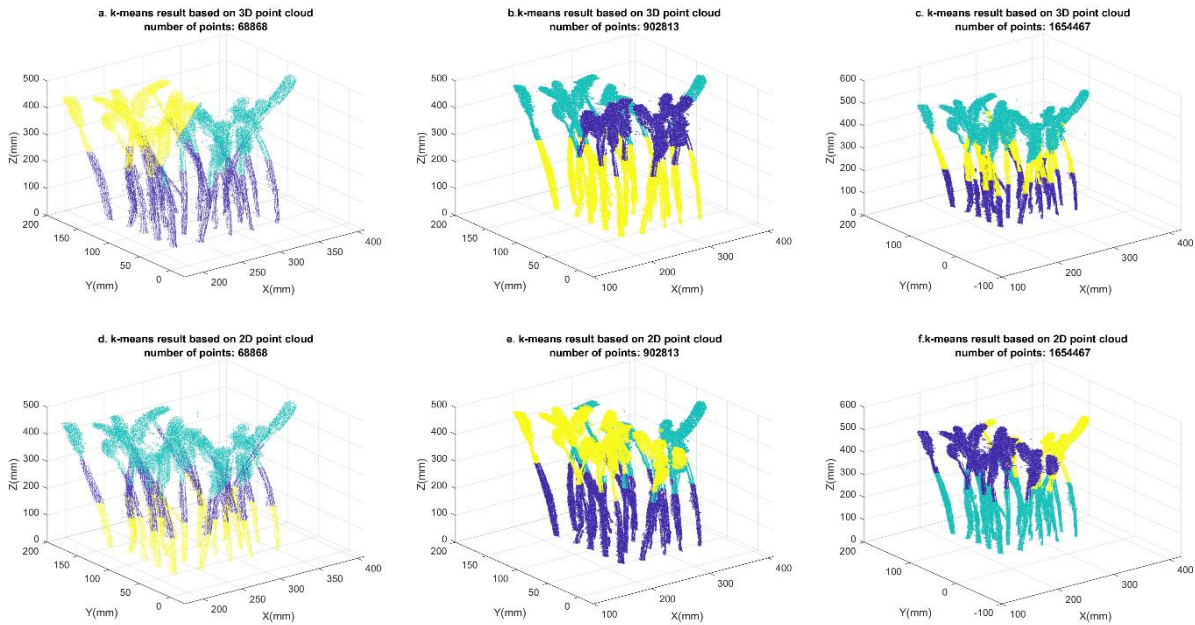
209 In this section, a series of 3D point cloud images captured from the laboratory was used to
210 test the performance of the proposed k -means algorithm. Five different field plots that were cap-
211 tured by our platform were selected and cropped to test the whole proposed measurement method.

212 *5.1. The analysis of the proposed k -means algorithm*

213 The proposed k -means algorithm is a two-stage method. In the first phase (Alg.1), the pro-
214 jection of a 3D point cloud image into a 2D point cloud (side view) is a dimension reduction
215 process. In order to test that this dimension reduction can not only output good results but also
216 improve the speed of the algorithm, some experiments were carried out and the results shown in
217 Fig. 10.

218

219



220

221

222

Fig. 10 -Results of *k*-means based on 3D and 2D point clouds.

Table 1 – The comparison running time between 3D and 2D point clouds.

Number of points	Running time of 3D point cloud	Running time of 2D point cloud
68868	1.91 s	1.67 s
902813	9.28 s	8.69 s
1654467	16.86 s	15.12 s

223

224

225

226

227

228

229

230

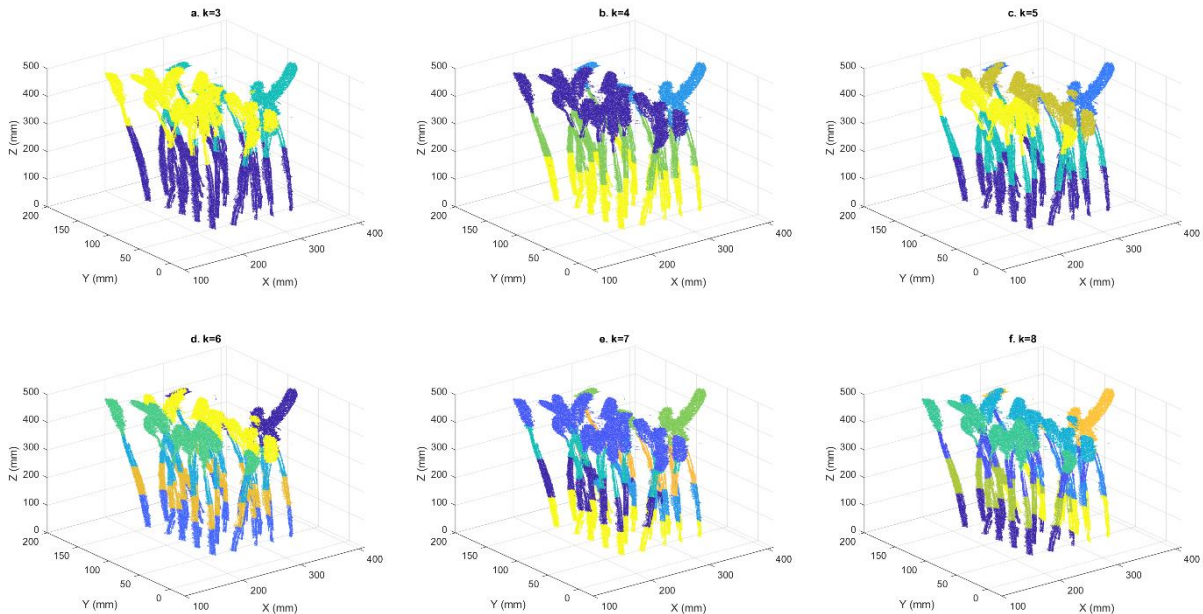
231

232

233

As shown in Fig. 10, for the same scene of the 3D point cloud, the number of points was adjusted by down sampling. The algorithm was run five times to calculate the average results that were implemented in MATLAB R2020b based on a Core i9-9980HK CPU 2.40GHz laptop. The comparison running time between 3D and 2D point clouds is shown in Table.1. It indicates that using *k*-means to process 3D and 2D point cloud images, the results were similar, but with the increase of points, the computational efficiency of the 2D point cloud was improved. Note that the running time included the whole time from loading the point cloud to drawing the resulting picture. Additional, the Lite *k*-means was used to obtain these results, compared with the traditional *k*-measure, Lite *k*-means process significantly improved the calculation speed by using the operation mechanism of MATLAB.

234 Further, in the first phase, the parameter (k) of k -means was not expected to have a great
235 impact on our expected result. To verify this, Fig. 11 shows the clustering results with different
236 values of k .



237

238

239

Fig. 11 – The clustering results with different values of k

240 Since the proposed algorithm only needs to preserve the top segments to obtain the spikes,
241 all of the results of Fig. 11 can be used, but if a small k value is selected, a portion of stems will
242 be considered as part of the top segments. This will introduce an error in spike height. If a bigger
243 value of k is chosen, the stem points counted might be less. However, it cannot be guaranteed
244 that there is a perfect parameter value to completely remove all of the stem's points. Also, as the
245 value of k increases, the efficiency of the algorithm might be reduced. This will be discussed in
246 the next section.

247 For the second phase (Alg.2), the projection of the 3D point cloud image onto the 2D point
248 cloud (top view) is more important. This is because the height of the spike is longer than the
249 width and length in 3D space, projecting the 3D image onto a 2D top view can reduce the point
250 distance in within-cluster, which can improve the algorithm to identify the individual spikes. To
251 validate the performance of this phase, different scenes were tested with the proposed algorithm.
252 As shown in Fig. 12, in these three scenes, some of the wheat crops were dense or mutually
253 overlapping (highlight areas), but from the clustering results, the proposed method still shows

254 some robustness and feasibility, especially compared with the traditional algorithm results in
255 section 2.1.

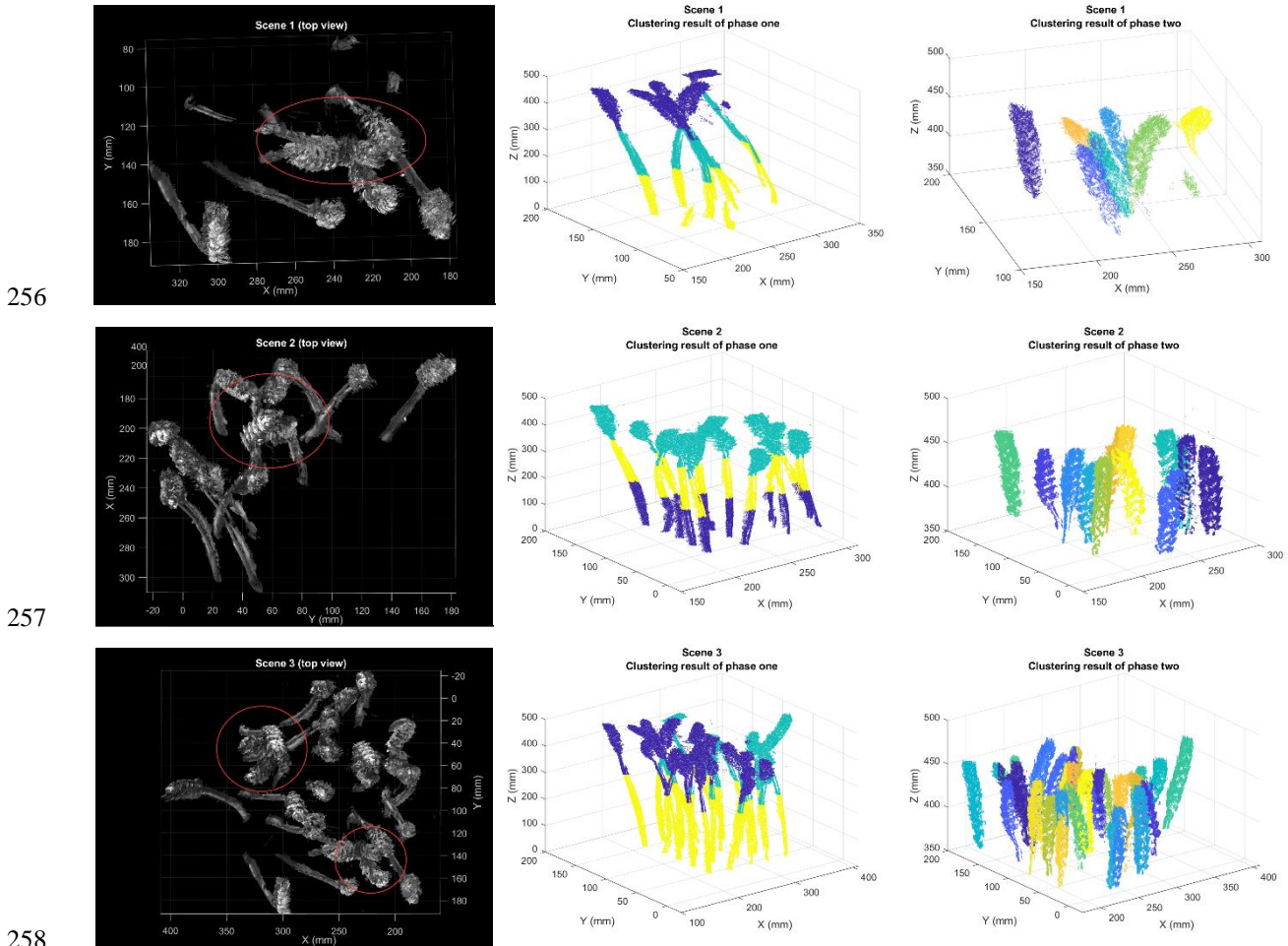


Fig. 12 – Clustering results with different scenes.

260 *5.2. The efficiency analysis of the proposed algorithm*

261 To analyse the efficiency of the algorithm, the same laptop mentioned above ran the algo-
262 rithms for different situations of the wheat crops. For the three situations in Fig. 12, the algorithm
263 was run 5 times for each situation and the average time recorded. The value of k was set as 6 for
264 phase one (Alg. 1) and max iterations of the RANSAC algorithm (in phase two) as 1,000. The
265 average running time of phase one and phase two is recorded separately in Table 2.

266

267

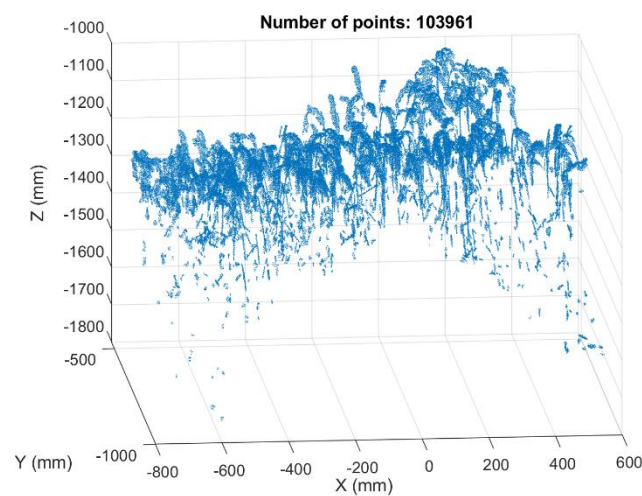
268

Table 2 – The average running time of the proposed algorithm.

Scene number	Number of points	Running time for phase one	Running time for phase two
1	166283	3.26 s	44.27 s
2	747982	8.84 s	184.13 s
3	902813	12.51 s	377.68 s

269

270 As can be seen from Table 2, thanks to the performance of Lite k -means, the k -means in the
271 proposed algorithm did not consume many computing resources. Comparing Table 1 with Table
272 2, the different parameter values that can influence the calculation time can be seen but the
273 changes are not large (in Table 1, k is 3). However, in phase two, the algorithm operates with
274 self-adaptive updating of the parameters and calls the RANSAC to fit the shape of each cuboid,
275 and this part plays a key role in the efficiency of the algorithm. Throughout the whole process,
276 the efficiency of the algorithm in processing wheat was good. Furthermore, the running time for
277 handling a field image was tested. The testing image is shown in Fig.13. For the volume calcu-
278 lation, the main calculation time was to divide all spikes into 3,000 segments, and the RANSAC
279 called to fit each segment to evaluate the total volume. Therefore, the parameter k was set as
280 3,000 to carry out the segmentation and then realise shape fitting. The whole running time was
281 36.7 minutes.



282

283

Fig. 13 – Example of a segment of field image for the run-time test.

284 According to the above experiments, it can be seen that the proposed method consumes
 285 most computing time when calculating the total volume of spikes. This is because the method
 286 needs to call the RANSAC 3,000 times to fit the shape of each small segment. Overall, the pro-
 287 posed algorithm can evaluate the sampled spike size with high efficiency. For the volume calcu-
 288 lation of spikes, using the proposed method, it takes about 30 to 40 minutes to complete the
 289 volume calculation once on a standard modern laptop.

290 5.3. Comparison of manual measurement with the proposed method

291 The method proposed in this paper can be applied to the scenario of hundreds of wheat
 292 crops. Therefore, this section describes experiments to validate the proposed method compared
 293 with manual measurement. Five different scenarios were tested with this method, each scenario
 294 is around one square metre of a wheat field, and the original images used are shown in Fig. 14.

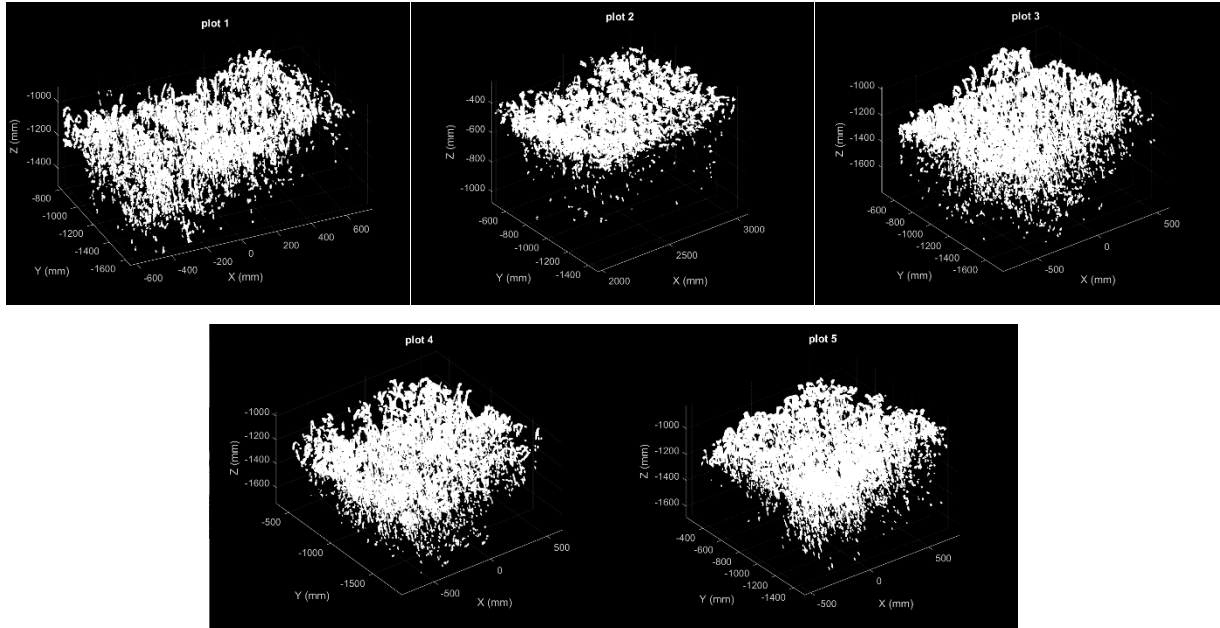
295 For manual measurement, a sample area is usually selected in the field. The number and
 296 size of spikes in the sample area are measured to infer the total number and average size of wheat
 297 crops in the entire field. In this experiment, for each scenario, we selected a 0.25 m² square as
 298 the sample area. The number of spikes n_m were counted and the average size of spikes (height
 299 h_m and width w_m) in the sample area was measured. The amount of wheat (spikes m⁻²) was cal-
 300 culated according to the following equation:

$$301 \quad num_m = \frac{n_m}{0.25} \quad (1)$$

302 The proposed method calculated all spike total volume V_a and the average size of the single
 303 spike. Note that Alg. 2 can output the height, length and width (h_a, l_a, w_a) of the spike and cuboid
 304 fitting was used to facilitate comparison with manual measurement. The values h_a and
 305 $w'_a = \frac{(l_a + w_a)}{2}$ were used to compare with h_m and w_m . As each tested scenario is about one
 306 square meter of a wheat field, for the proposed method, spikes total volume was divided by the
 307 single spike volume to estimate the number of spikes in each scenario according to the following
 308 equation:

$$309 \quad num_a = \frac{V_a}{h_a \times w'_a \times w'_a} \quad (2)$$

310



311

312

Fig. 14 – Five different 3D point field images from the field.

313 The comparison results are recorded in Table 3. To compare the proposed method with the
 314 manual method, the following equations were used to estimate the error rate of each plot:

315 Error rate in the number of spikes: $Error_1 = \frac{|num_m - num_a|}{num_m}$ (3)

316 Error rate in the spike height: $Error_2 = \frac{|h_m - h_a|}{h_m}$ (4)

317 Error rate in the spike width: $Error_3 = \frac{|w_m - w_a|}{w_m}$ (5)

318 As we can see in Table 4, in the five experiments, the three average error rates defined
 319 above were 16.27%, 5.24% and 12.38% respectively.

320

321

322

Table 3 – Comparison results between manual measurement and the proposed method.

Plot number	Average size		Number of spikes		Total volume V_a
	Manual	Proposed method	Manual	Proposed method	
	h_m/w_m	h'_a/w'_a	num_m	num_a	
1	83.4/13.5 mm	76.7/12.4 mm	212	173	2042491 mm ³
2	71.9/15.5 mm	63.6/14.6 mm	260	202	2766830 mm ³
3	84.2/14.2 mm	81.8/18.2 mm	200	259	7020030 mm ³
4	82.4/15.2 mm	81.3/17.6 mm	212	207	5179640 mm ³
5	78.3/15.0 mm	76.4/15.6 mm	228	208	3866860 mm ³
Standard Deviation	5.1/0.8 mm	7.4/2.3 mm	/	/	/

323

324

Table 4 – Error rates of the proposed method.

Plot Number	$Error_1$	$Error_2$	$Error_3$
1	18.40%	8.03%	8.15%
2	22.31%	11.54%	5.81%
3	29.5%	2.85%	28.17%
4	2.36%	1.34%	15.79%
5	8.77%	2.43%	4%
Average	16.27%	5.24%	12.38%

325

326 5.4. Discussion

327 From all of our experiments, we made a detailed analysis of the proposed k -means algorithm.
328 Although k -means is an uncertain algorithm that cannot guarantee that the output is always the
329 same, for our proposed algorithm the clustering result was good enough for shape fitting. Addi-
330 tionally, the shape fitting algorithm is not the focus of this paper although it was discovered by
331 using the cuboid fitting that the fitting result for straight spikes was better than for the curved
332 ones. This is because cuboids cannot accurately fit the height of curved wheat spikes. Further-
333 more, as shown in Table 3, all of the average heights obtained by the proposed algorithm were
334 slightly smaller than that measured manually. This was because most of the tested wheat spikes
335 were slightly curved, and there would be some errors when using cuboid shape fitting. Besides

336 the shape fitting algorithm, with the spikes being more curved, the overlapping in the plan view
337 will be obvious. This might influence the clustering result of the proposed k -means algorithm.

338 Further, there are still a few issues in our method which might be considered to address in
339 future work. First, a self-adaptive k -means algorithm to update the k iteratively in Alg.2 was
340 proposed for spikes counting. However, for volume calculation, the computational efficiency
341 was not very good. Therefore, when we dealt with the field images, we divide the whole image
342 into three segments. Secondly, as mentioned above, the accuracy of this method was affected by
343 the curvature of the spike. Five field data set results were used and the average error in the num-
344 ber of spikes was greater than 16%, of which two errors were greater than 20%. The performance
345 of the algorithm might decrease if this analysis was extended to spike dimensions assessment for
346 other field data sets.

347 Overall, all of the experiment results imply that our method has a good potential to be de-
348 veloped as a tool to evaluate the size and yield of wheat spikes, especially for straight spikes,
349 whilst avoiding the time-consuming and tedious manual measurements.

350 **6. Conclusion**

351 A high-throughput field capture platform for wheat combined with an unsupervised auto-
352 matic measurement of wheat spikes based on an adaptive k -means algorithm with dynamic per-
353 spectives is proposed, which can deal with the complex environment where hundreds of wheat
354 spikes are grown densely. This method has provided a novel framework to obtain wheat spike
355 dimensions and total volume in the place of manual measurement. The results demonstrate a
356 level of robustness of our method to measure the wheat spike dimensions and volume in the
357 wheat field scenario. As method performance can still be improved to handle curved wheat
358 spikes, our future work will further optimise our algorithm to deal with the environment where
359 the wheat spike is arched.

360 **ACKNOWLEDGMENTS**

361 This work is supported by the UK Government's Department of Business, Energy and In-
362 dustrial Strategy (BEIS) as part of the National Measurement System (NMS) programme.

363

References

- Cai, D. (2011). *Litekmeans: the fastest matlab implementation of kmeans*. Software Available at: [Http://Www.zjucadcg.cn/Dengcai/Data/Clustering.html](http://www.zjucadcg.cn/Dengcai/Data/Clustering.html)
<http://www.cad.zju.edu.cn/home/dengcai/Data/code/litekmeans.m>
- Deery, D., Jimenez-Berni, J., Jones, H., Sirault, X., & Furbank, R. (2014). Proximal remote sensing buggies and potential applications for field-based phenotyping. In *Agronomy*. <https://doi.org/10.3390/agronomy4030349>
- Ester, M., Kriegel, H.-P., Sander, J., & Xu, X. (1996). A Density-Based Algorithm for Discovering Clusters in Large Spatial Databases with Noise. *Proceedings of the 2nd International Conference on Knowledge Discovery and Data Mining*.
- Fernandez-Gallego, J. A., Kefauver, S. C., Gutiérrez, N. A., Nieto-Taladriz, M. T., & Araus, J. L. (2018). Wheat ear counting in-field conditions: High throughput and low-cost approach using RGB images. *Plant Methods*. <https://doi.org/10.1186/s13007-018-0289-4>
- Lai, W., Zhou, M., Hu, F., Bian, K., & Song, Q. (2019). A New DBSCAN Parameters Determination Method Based on Improved MVO. *IEEE Access*, 7, 104085–104095. <https://doi.org/10.1109/ACCESS.2019.2931334>
- Li, Lei, Zhang, Q., & Huang, D. (2014). A review of imaging techniques for plant phenotyping. In *Sensors (Switzerland)*. <https://doi.org/10.3390/s141120078>
- Li, Lingxiao, Sung, M., Dubrovina, A., Yi, L., & Guibas, L. J. (2019). Supervised fitting of geometric primitives to 3D point clouds. *Proceedings of the IEEE Computer Society Conference on Computer Vision and Pattern Recognition*. <https://doi.org/10.1109/CVPR.2019.00276>
- Mohamed, I., & Dudley, R. (2019). Comparison of 3D Imaging Technologies for Wheat Phenotyping. *{IOP} Conference Series: Earth and Environmental Science*, 275, 12002. <https://doi.org/10.1088/1755-1315/275/1/012002>
- Pask, A., Pietragalla, J., & Mullan, D. (2012). Physiological Breeding II: A Field Guide to Wheat Phenotyping. In *Chemistry & ...*
- Rolf Harkes. (2018). *GitHub - rharkes/DBSCAN-for-Matlab: using kd-trees*. <https://github.com/rharkes/DBSCAN-for-Matlab>
- Sadeghi-Tehran, P., Virlet, N., Ampe, E. M., Reyns, P., & Hawkesford, M. J. (2019). DeepCount: In-Field Automatic Quantification of Wheat Spikes Using Simple Linear Iterative Clustering and Deep Convolutional Neural Networks. *Frontiers in Plant Science*. <https://doi.org/10.3389/fpls.2019.01176>
- Schnabel, R., Wahl, R., & Klein, R. (2007). Efficient RANSAC for point-cloud shape detection. *Computer Graphics Forum*. <https://doi.org/10.1111/j.1467-8659.2007.01016.x>
- Su, H., Jampani, V., Sun, D., Maji, S., Kalogerakis, E., Yang, M. H., & Kautz, J. (2018). SPLATNet: Sparse Lattice Networks for Point Cloud Processing. *Proceedings of the IEEE Computer Society Conference on Computer Vision and Pattern Recognition*. <https://doi.org/10.1109/CVPR.2018.00268>
- Tan, C., Zhang, P., Zhang, Y., Zhou, X., Wang, Z., Du, Y., Mao, W., Li, W., Wang, D., & Guo, W. (2020). Rapid Recognition of Field-Grown Wheat Spikes Based on a Superpixel Segmentation Algorithm Using Digital Images. *Frontiers in Plant Science*, 11, 259. <https://doi.org/10.3389/fpls.2020.00259>
- Thompson, A., Livina, V., Harris, P., Mohamed, I., & Dudley, R. (2019). Model-based algorithms for phenotyping from 3D imaging of dense wheat crops. *2019 IEEE International Workshop on Metrology for Agriculture and Forestry, MetroAgriFor 2019 - Proceedings*. <https://doi.org/10.1109/MetroAgriFor.2019.8909214>
- Torres, A., & Pietragalla, J. (2012). Crop morphological traits. In *Physiological Breeding II: A Field Guide to Wheat Phenotyping*.
- Velumani, K., Oude Elberink, S., Yang, M. Y., & Baret, F. (2017). WHEAT EAR DETECTION in PLOTS by SEGMENTING MOBILE LASER SCANNER DATA. *ISPRS Annals of the Photogrammetry, Remote*

Sensing and Spatial Information Sciences. <https://doi.org/10.5194/isprs-annals-IV-2-W4-149-2017>

- Wang, F., Mohan, V., Thompson, A., & Dudley, R. (2020). Dimension fitting of wheat spikes in dense 3D point clouds based on the adaptive k-means algorithm with dynamic perspectives. *2020 IEEE International Workshop on Metrology for Agriculture and Forestry, MetroAgriFor 2020 - Proceedings*. <https://doi.org/10.1109/MetroAgriFor50201.2020.9277611>
- Xia, S., Peng, D., Meng, D., Zhang, C., Wang, G., Gien, E., Wei, W., & Chen, Z. (2020). A Fast Adaptive k-means with No Bounds. *IEEE Transactions on Pattern Analysis and Machine Intelligence*. <https://doi.org/10.1109/tpami.2020.3008694>

Editor-in-Chief:

Thank you for making the changes required by the reviewers. Your paper is basically acceptable for publication but requires minor changes.

I have carried out a technical edit on your submission using Word Track Changes and suggested changes. You may access my edited version in the attachment. Please check my edits carefully as I may not have always understood your original meaning.

Please also check my comments.

I also suggest that you carefully examine the journal Guide for Authors available through the journal web site.

I look forward to shortly receiving a revised manuscript and moving to accept it for publication.

[Thanks for your consideration and for editing this article. Now we have accepted all of your edits and made changes according to your comments.](#)